Physicochemical characterization of a diatomaceous upon an acid treatment: a focus on surface properties by inverse gas chromatography

Tassadit Benkacem, Boualem Hamdi, Alain Chamayou, Henri Balard, Rachel Calvet

Physicochemical characterization of a diatomaceous upon an acid treatment: a focus on surface properties by inverse gas chromatography

Tassadit Benkacem [a,*], Boualem Hamdi [b,c], Alain Chamayou [d], Henri Balard [e], Rachel Calvet [d]

[a] Laboratoire de Génie Chimique, Université de Saad Dahleb 1, Route de Soumaa, BP 270, Blida, Algeria
[b] Ecole Nationale Supérieure des Sciences de la Mer et de l'Aménagement du Littoral ENSSMAL, Campus Universitaire de Dely Ibrahim, Bois des Cars, BP19, Alger 16320, Algeria
[c] Lab. d'Etude Physico-Chimique des Matériaux et Application à l'Environnement, Fac. de Chimie, USTHB, BP 32, El Alia, Bab Ezzouar, 16111 Alger, Algeria
[d] Université de Toulouse, Mines Albi, CNRS UMR 5302, Centre RAPSODEE, Campus Jarlard, F-81013 Albi cedex 09, France
[e] Adscientis, 1 rue Kastler 68310 Wittelsheim, France

A B S T R A C T

Natural diatomite from Sig/Algeria was treated with 0.5, 1.0, 3.0 and 5.0 M nitric acid solutions for 2 h under reflux at 333 K in order to improve its performance as support of catalyst. The purified silica powders obtained from frustules can also be used to reinforce composites. The solids obtained were characterized by scanning electron microscopy (SEM), X-ray diffraction (XRD), X-ray fluorescence (XRF), Fourier transform infrared (FTIR) spectroscopy, thermal analyses, and nitrogen adsorption–desorption at 77 K. Treatment of diatomite earth with nitric acid reduced mineral impurities, such as Fe_2O_3 and alkali metal oxides (CaO, MgO), eliminated carbonates and increased SiO_2 ratio from 88% to 98%. The SEM micrographs showed the original geometry of the pores to be preserved. The surface properties were also evaluated using inverse gas chromatography at infinite dilution (IGC-ID) and finite concentration (IGC-FC). The interest here was to establish whether the technique is sufficiently sensitive to detect variations in the surface properties of the diatomite due to this chemical treatment. The IGC analysis permitted to reach several surface energy components with organic probes. Between them, the distribution function of the adsorption energy sites obtained with the isopropanol probe revealed a silica structure after the 5 M nitric acid treatment.

Keywords:
Diatomite
Acid treatment
Inverse gas chromatography
Catalyst support

1. Introduction

Diatomaceous also known as diatomaceous earth, kieselguhr, tripolite, etc. is a siliceous sedimentary rock mainly made from the skeletons of aquatic plants or algae called diatoms [1] Amorphous silica, a constituent of the diatom frustules, is the main component of diatomite, although variable quantities of impurities such as metal oxides, mineral clays, salts (mainly carbonates) and organic matter may also be present [2,3]. The diatom shell has properties such as a high porosity with a strong adsorption ability and an excellent thermal resistance related to physical structures and aggregates of fine particles perforated by regular pattern of very small holes. Hence, diatomite has been widely used as filter aid, pharmacy carrier and adsorbent [2–4].

The abundance and availability of these mineral reserves as a raw material source and their relatively low cost guarantee their continued utilization in the future. Recently the diatomite was examined as a perfect support material in preparation of solid catalysts [5]. The main features of a catalyst support according to Satterfield [6] are its chemical nature which is defined by the acidic or basic character of the surface depending on physical or chemical treatments they have received and the presence of impurities in the catalyst quarry. Similar to the synthetic amorphous silica, the reactivity of diatomite is linked to the presence of reactive sites on its surface such as hydroxyl groups which are the main reactive sites. Apart from the hydroxyl groups, acid sites as iron or aluminum oxides are also considered as important sites on the surface of diatomite [7]. But the presence of impurities such as clay, carbonate calcium on the diatomaceous surface limits the use of this material.

There are several methods to modify the surface characteristics of clays minerals for various purposes. Acid treatment is usually employed for improving surface properties of diatomite. The aim of acid treatment is to eliminate impurities such as carbonate groups, which are inhibitors of photocatalytic reactions implementing hydroxyl ions. Indeed hydroxyl ions are trapped by carbonates and lead to radicals less reactive. On the other hand, carbonates can fill the natural pores of the diatomite. So an other interest of removing carbonates is to open these blocked pores and to increase the specific surface area of the diatomite, the performance of a catalyst being directly related to the specific surface area. Extensive studies were carried out in order to evaluate the effect of acid treatments on the porous texture or structure [8,9].

The present investigation sets out the influence of nitric acid treatment on a diatomaceous silica sample, with the aim of its valorization

* Corresponding author.
E-mail addresses: bnihaya@yahoo.fr (T. Benkacem), bhamdi_99@yahoo.fr (B. Hamdi), alain.chamayou@mines-albi.fr (A. Chamayou), h.balard@wanadoo.fr (H. Balard), rachel.calvet@mines-albi.fr (R. Calvet).

as a catalyst support. Different methods, such as X-ray diffraction, Fourier transform infrared spectroscopy, scanning electron microscopy were used to characterize the variation of the diatomite properties before and after treatments with different concentrations of nitric acid. Inverse gas chromatography (IGC) was also carried out; it is now a well-established technique for the study of surface properties, extensively applied for characterization of various finely divided powders, mineral fillers, pigments, silicates [10,11], composite materials [12], organic materials such as plastics, textiles, food or pharmaceutic solids [13], etc. With this technique, the surface characterization of the solids is performed by injecting probes of known properties into a column containing the solid of interest. The retention time or the retention volume of these probes, measured near zero surface coverage, allows the determination of interactions, including London (i.e. apolar) and specific (i.e. polar) interactions, established between the probes and the solid and then the characterization of the solid surface. In a second time, if the solid surface is entirely covered with a probe monolayer, a distribution function of adsorption sites can be determined.

2. Theory on inverse gas chromatography

Depending on the amount of probe molecules injected into the chromatographic column, IGC may be performed at infinite dilution (IGC-ID) [14], but also at finite concentration conditions (IGC-FC) [15,16].

2.1. Inverse gas chromatography at infinite dilution (IGC-ID)

This technique consists in filling a column with the solid under test and in injecting very small amount of probe molecules (vapor) with known properties (length of the carbon atoms chain, polarity, ramification), at the limit of the detector sensitivity. Depending on the chemical nature of the probe and its geometry, the three following parameters can be determined:

- The dispersive component of the surface energy, obtained by injections of a n-alkanes series [17]. This parameter gives a measurement of the non-specific interactions that is to say London forces developed between the probes and the solid surface.
- The nanomorphological index, determined by injections of branched or cyclic alkanes. This index delivers information about the surface roughness of the solid at the scale of the injected probe [18,19].
- The specific interaction parameters, established by injections of polar probes, that give access to polar interactions, mainly the acid–base interactions [19].

2.2. Inverse gas chromatography at finite concentration (IGC-FC)

In IGC-FC, a few microliters of a liquid probe are injected into the column containing the solid to be analyzed, in order to cover entirely with a molecule mono-layer the solid surface. A strong asymmetric chromatographic peak is obtained when ideal, nonlinear conditions are fulfilled.

IGC-FC permits the access to desorption isotherms of the probe molecule [15,21]. The simplest method, from the point of view of the analysis duration, is “the elution characteristic point method” (ECP) that allows the acquisition of part of the desorption isotherm from a unique chromatographic peak. According to this method, the first derivative of the isotherm is related to the retention time for each point of the rear diffuse profile of the chromatogram by the Conder's Eq. (1):

$$\left(\frac{\partial N}{\partial P}\right)_{L,t_r} = \frac{JD}{mRT}(t_r - t_0) \tag{1}$$

where N is the number of desorbed molecules, P the partial pressure of the probe at the output of the column, L the column length, t_r the retention time of a characteristic point on the rear diffuse profile of the chromatogram, t_0 the retention time of CH_4, D the flow rate at the output of

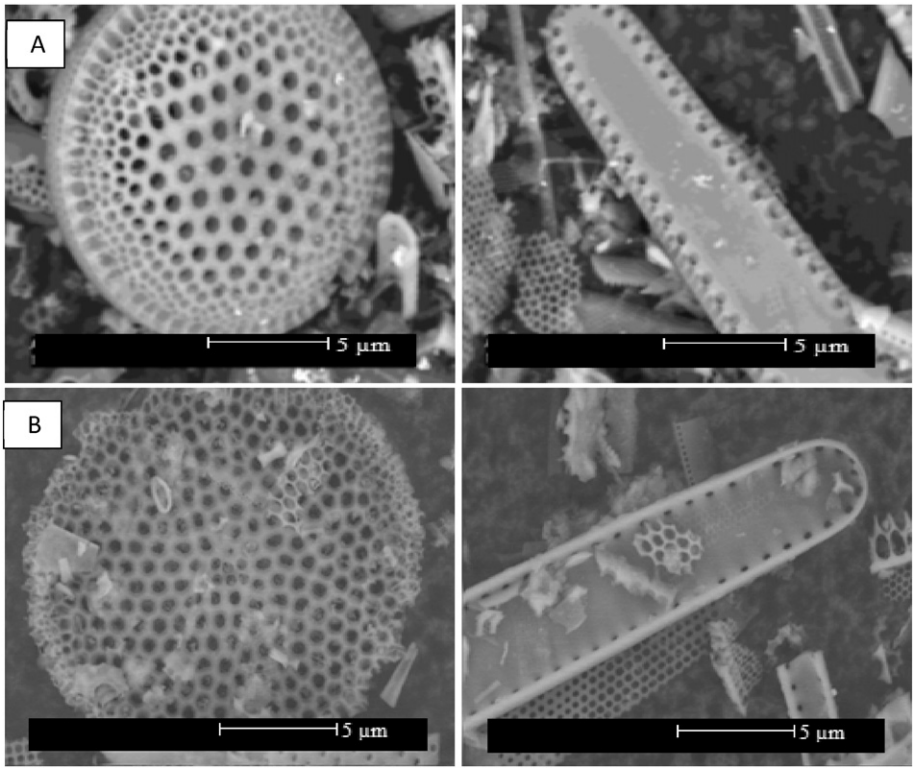

Fig. 1. SEM micrographies of (A) raw diatomite and (B) diatomite after 2 h with HNO_3 0.5 M.

the column, J the James–Martin correction factor, m the mass of adsorbent, R the perfect gas law constant, and T the oven temperature.

After integration of Eq. (1), the desorption isotherm of the probe can be obtained, from each point of the rear diffuse profile of the chromatogram, the pressure of the probe being directly related to the height of the signal. Several information may be extracted from the isotherm such as the Henry's constant, the specific surface area and the BET constant for different organic probes.

Due to the presence of adsorption sites having high energy interactions, a non-negligible part of the injected probe is not eluted in time corresponding to the return of the signal to the baseline. In order to assess the amount of irreversibly adsorbed probe on the surface, the temperature of the chromatograph oven is increased up to the conditioning temperature, leading to appearance of a secondary small peak.

An irreversibility index, I_{irr}, is defined from the ratio of the thermodesorption peak area onto the total area of the chromatogram [20], and computed according to Eq. (2):

$$I_{irr} = \frac{S_{th}}{(S_{rv} + S_{th})} \tag{2}$$

where S_{rv} is the surface of the main chromatographic peak and S_{th}, the surface corresponding to the thermodesorption peak.

Also, the shape of the desorption isotherm is influenced by the surface heterogeneity; molecules adsorbed on the sites having the highest energy will remain a longer time in the chromatographic column than those visiting the sites of lower energy. Hence, the analysis of the isotherm shape will permit to access to the distribution function of the adsorption energies (DFAE).

Estimation of the surface heterogeneity of a solid through the DFAE is generally based on a physical adsorption model which admits that the global isotherm may be considered as a sum of local isotherms of adsorption on isoenergetic domains (patchwork model) [16,21,22]. Then, the surface heterogeneity is described by a distribution function corresponding to the relative abundance of each type of domains having the same characteristic energy of interaction (ε) as shown in Eq. (3):

$$N(T,P) = N_0 \int_{\Omega} \theta(\varepsilon, T, P)\chi(\varepsilon)d\varepsilon \tag{3}$$

where $N(T,P)$ is the number of molecules adsorbed at the pressure P and the temperature T, N_0 is the number of molecules which can form a monolayer, θ (ε,T,P) is the local isotherm corresponding to adsorption sites having the same characteristic adsorption energy ε, $\chi(\varepsilon)$ is the so-called distribution function of the adsorption energies (DFAE) describing the energies which exist at the gas–solid interface, Ω is the physical domain of the adsorption energy, and ε is the characteristic energy.

Comparing the computed distribution function (DF) with the DF describing an homogeneous surface that fits the left descending branch of the experimental DF towards the lowest interaction energies [20], allows to calculate an index of surface heterogeneity, I_{hete}, defined in Eq. (4):

$$I_{hete} = \frac{A - A_H}{A} \tag{4}$$

where A is the area under the experimental DF and A_{H} the area under the homogeneous DF.

The distribution functions were computed using special software from the ADSCIENTIS society (Wittelsheim, France).

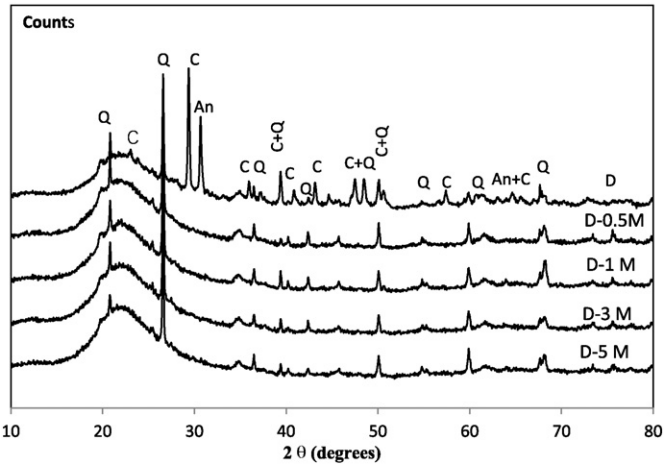

Fig. 2. X-Ray patterns of diatomite before and after acid treatments at different nitric acid concentrations (Q: quartz, C: calcite (CaCO3), An: ankerite Ca(Mg,Fe)(CO3)2).

3. Experimental

3.1. Materials

In this study, diatomite, containing silica more than 88% by weight, was obtained from the region of Sig, at the north west of Algeria. The raw diatomite was first crushed and sieved to obtain a size fraction between 100 and 200 μm, allowing easier analysis. The nitric acid used for the acid treatment was provided by the Merck Company and had a 68% purity. The probes employed for IGC were apolar alkanes: n-pentane (C5), n-hexane (C6), n-heptane (C7); a branched alkanes: 2,5-dimethylhexane (2,5-DMH) and 2,3,4-trimethylpentane (2,3,4-TMP); cyclic alkanes: cycloheptane (Cy7) and cyclooctane (Cy8); and polar probes (chloroform $CHCl_3$, dichloromethane CH_2Cl_2, isopropanol (IP) and 1,4-dioxane (DX). These probes had chromatographic grade (>99%) purity.

3.2. Acid treatment of diatomite

The acid treatment of diatomite was carried out by adding 50 g of diatomite to 500 mL of nitric acid solutions with different concentrations (0.5, 1.0, 3.0 and 5.0 M) and refluxing at 300 K in round bottomed flask equipped with a reflux condenser for 2 h. The nitric acid was preferred to hydrochloric acid because with the latter, chlorinated residues can form toxic dioxins with Persistent Organic Pollutants when photodegradation occurs. The content was filtered, then repeatedly

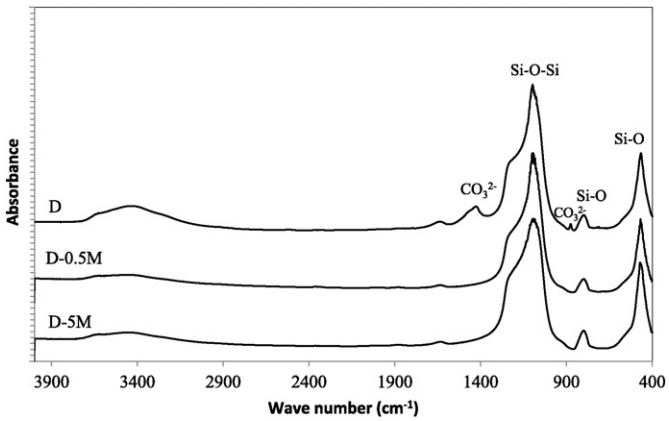

Fig. 3. IR spectra of diatomite before and after treatments with 0.5 M and 5 M nitric acid, in 3900–400 cm^{-1} region.

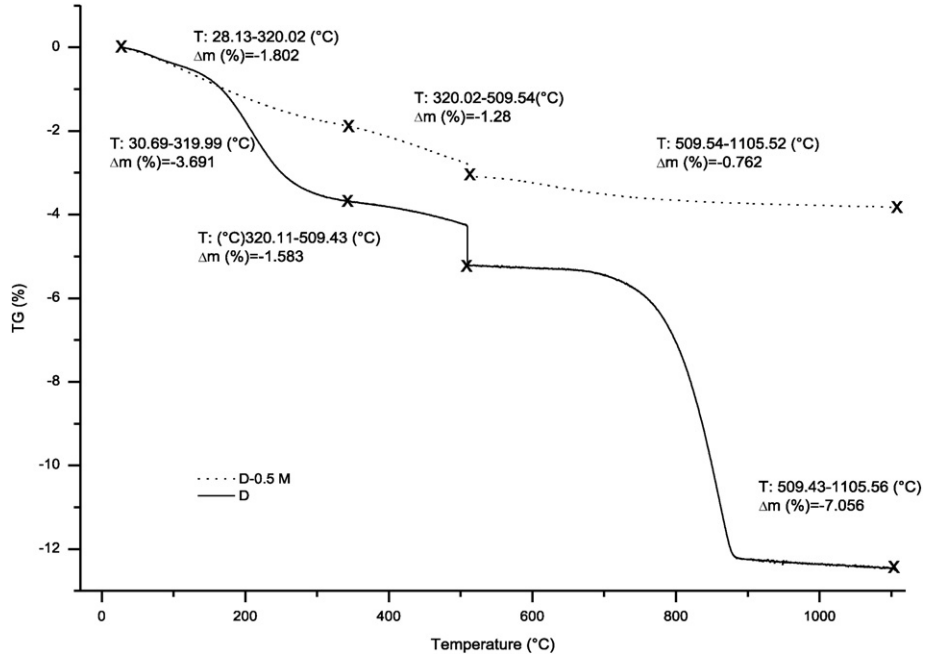

Fig. 4. Thermogravimetric curves of raw diatomite (solid line) and D-0.5 M (dotted line).

washed with distilled water to remove any unspent acid, and dried in an oven at 373 K overnight, before characterizations. In the following text, the letter D is referred to the untreated diatomite sample and D-0.5 M, D-1 M, D-3 M, and D-5 M to the treated samples with the numbers indicating the different acid concentrations.

3.3. Characterization methods

Particles morphology was investigated using a scanning electron microscope (Philips XL 30 model ESEM-FEG) operating at 8 kV.

X-ray diffractograms were obtained using a PANanalytical X'Pert Pro MPD diffractometer (set-up Bragg–Brentano). Diffraction data were acquired by exposing the powders samples to Cu–Kα radiation, which has a wavelength of 1.5418 Å. The generator was set to 45 kV and to a current of 40 mA. The data were collected over a range of 5°–80° 2θ with a step size of 0.03° 2θ and a nominal time per step of 100 s, using the scanning X'Celerator detector. Data analysis was performed using X'Pert Data Collector software and phase identification was carried out by means of PANalytical High Score Plus software in conjunction with the ICDD Powder Diffraction File 2 database and the Crystallography Open Database.

Chemical composition analysis was established by a Epsilon 3XL X-ray fluorescence (XRF) spectrometer (PANalytical).

The density of the solids was measured using a helium displacement method with an AccuPyc 1340 pycnometer (Micromeritics).

The specific surface areas and BET constants were determined from nitrogen adsorption isotherms obtained at 77 K with an ASAP 2010 apparatus (Micromeritics). The samples were previously out gassed at 383 K until a relative pressure of less than 10^{-5} Pascal.

The FTIR spectra of the samples were obtained using a Fourier transform infrared (FTIR) spectrophotometer (Perkin Elmer 2000) with a resolution of 4 cm^{-1} and a scan number equal to 4. The spectral study was extended over the range 4000–400 cm^{-1}. The analysis was done by transmission on KBr pellets with 1% of sample, prepared using a hydraulic press by applying a pressure of 10 kPa.

Thermogravimetric analysis (TG) was performed on a Setaram TG-ATD 92 instrument. The heating range was from 303 to 1373 K at a heating rate of 5 °C/min under nitrogen atmosphere.

The IGC measurements were carried out on an Agilent GC 6890 gas chromatograph, equipped with highly sensitive flame ionization detectors (FID). Helium was used as the carrier gas with a flow rate of 30 mL/min measured with an electronic flow meter (Flow 500-Agilent). The injector and detector were respectively heated to 423 K and 443 K. The columns were stainless steel tubes of 6.35 mm inside diameter and 10 cm length, filled with a sample mass between 0.32 and 0.42 g. All the columns were conditioned at 180 °C overnight to eliminate the water adsorbed on the surface. The conditioning temperature was chosen after a study made on the effect of temperature on the surface properties of the diatomite; until 453 K, the surface properties of the solid were not altered.

Table 1
Chemical composition of raw and acid treated diatomite at different nitric acid concentrations determined by XRF.

Elements (%)	Chemical composition				
	D	D-0.5 M	D-1 M	D-3 M	D-5 M
SiO_2	87.87 ± 1.63	96.44 ± 0.93	97.00 ± 0.72	97.2 ± 0.28	97.97 ± 0.69
CaO	9.04 ± 0.59	0.18 ± 0.07	0.15 ± 0.02	0.11 ± 0.05	0.13 ± 0.01
Al_2O_3	1.97 ± 0.15	1.78 ± 0.44	1.51 ± 0.2	1.59 ± 0.29	1.65 ± 0.39
Fe_2O_3	1.51 ± 0.28	1.12 ± 0.57	0.97 ± 0.01	0.63 ± 0.00	0.33 ± 0.29
K_2O	0.48 ± 0.08	0.49 ± 0.10	0.47 ± 0.05	0.42 ± 0.04	0.42 ± 0.03
TiO_2	0.12 ± 0.04	0.16 ± 0.03	0.15 ± 0.02	0.15 ± 0.02	0.15 ± 0.01
MgO	0.83 ± 0.12	0.16 ± 0.15	0.21 ± 0.05	0.22 ± 0.12	0.15 ± 0.03
Fe/Si	0.010	0.006	0.006	0.004	0.002

The values after the sign (±) is the standard deviation obtained from five measurements for the raw diatomite and three ones for the acid treated samples.

The IGC-ID study was done with an oven temperature of 373 K. This temperature was set so as to allow a return to the baseline between different peaks (methane and probes). Dead time, t_0, was determined by a non-adsorbed molecule namely Methane. The probes used were linear, branched or cyclic alkanes and polar ones (dichloromethane and chloroform).

In IGC-FC, analysis temperatures depended on the probe used, according to the Conder criterion [15], which states that the contribution of probe vapor to the total flow of carrier gas at the maximum of the chromatographic peak should not exceed 5% of the initial flow. Whatever the probe injected, apolar or polar, the interactions with the diatomite surface were very strong, leading to very long analyses in IGC-FC between 12 and 15 hours. To minimize the duration of analyses by increasing the temperature analysis, contribution of 7.1% was accepted. Three probes were examined, an apolar one, the octane (C8) at 343 K, which is mainly sensitive to the surface morphology, and two polar ones, the isopropanol at 323 K and the 1,4-dioxane at 333 K which are more sensitive to the surface functionality, especially the presence of silanol groups.

The injections of each probe were repeated three times and three columns were made with each sample for taking into account the heterogeneity of the solid. The quantities after the sign (±) in the values tables correspond to the standard deviation from duplicate measurements.

4. Results and discussion

4.1. Morphological, chemical and textural characterizations

4.1.1. Analysis of morphology and microstructure

Examination of the samples with SEM confirms that the diatomite particles consist of various types of morphologies (Fig. 1). There is a nearly regular array of submicron pores from 200 nm to 1 μm diameters. The original geometry of the pores and morphology seem to be preserved after the acid-leaching.

After the observation of the particles morphology by SEM, it would be interesting to investigate the influence of the acid treatment on the chemical composition of the diatomite.

4.1.2. Analysis of the chemical structure

The X-ray analysis of the diatomite powder before acid treatment is given in Fig. 2. No characteristic peaks were detected over a 2θ range of 5°–10°, that's the reason why the data are presented over a range of 10°–80° (2θ). It shows essentially an amorphous silica phase, revealed by a large peak between 16° and 26° (2θ), but also quartz and carbonates like calcite and ankerite. From the treatment with the 0.5 M HNO_3 concentration, all the carbonates disappear and also remain the amorphous silica and crystalline quartz. This result agrees with literature data that acid treatment does not change the diatomite structure and quartz significantly [24].

The IR analysis spectra are gathered in Fig. 3. Before the acid treatment, the broad band between 3000 and 3800 cm^{-1} and the one at 1637 cm^{-1} are attributed respectively to –OH stretching and bending vibrations of the physically adsorbed water molecules [7]. The first one broad band probably covers the peaks corresponding to vibrations of different hydroxyl groups of the diatomite (single or germinal, H-bonded or isolated ones) [7]. The peaks around 1100 cm^{-1} are assigned to the Si–O–Si stretch vibrations. Other bands at 795 cm^{-1} and 474 cm^{-1} are also characteristic of silica [23]. Upon the effect of the 0.5 M HNO_3 treatment, the carbonates IR bands found at 875 cm^{-1} and 1426 cm^{-1} are eliminated corroborating the results of X-ray analysis. However, above the 0.5 M HNO_3 concentration, the characteristic bands of diatomite structure remain unchanged.

The thermogravimetric analysis of the raw diatomite powder is given in Fig. 4. It exhibits three main mass losses. The first mass loss of 3.7% of the initial mass in the range of 304–593 K is attributed to the desorption of physisorbed water. The second mass loss (1.6%) in the range of 593–783 K should be attributed to dehydroxylation of calcium hydroxide. The third mass loss, the more important in percentage, 7.1%, at the temperature range 783 K to 1373 is ascribed to decarbonation. This last one disappears for the sample treated with 0.5 M HNO_3 concentration, emphasizing one more time that this concentration is sufficient to eliminate carbonates.

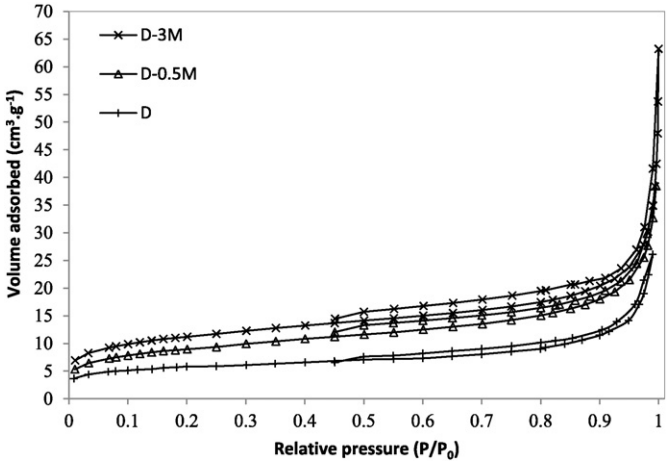

Fig. 5. Nitrogen adsorption–desorption isotherms of raw and acid treated diatomite samples respectively denoted as D, D-0.5 M and D-3 M.

The quantification of chemical compositions of the natural and acid treated diatomite will help us to precise the variation of diatomite structure treated with different acid concentrations.

The chemical compositions of the natural and acid treated diatomite samples expressed as weight percentage are reported in Table 1. As can be seen, The XRF results show that the main components of the natural raw diatomite are Si and Ca oxides, with few amounts of the Al_2O_3, MgO, and F_2O_3 contents. After the acid treatment, the SiO_2 ratio increases, at the same time as the CaO, MgO, and F_2O_3 contents decrease. The increase of SiO_2 ratio can be ascribed to the fact that the silica is relatively resistant to acid attack whereas Mg and Fe salts are more soluble in acidic conditions [3]. Calcium is mainly in the form of carbonate, which can be decomposed easily in acidic media. Thus, the content of CaO decreased markedly after acid of low concentration was added.

XRF also gives evidence that the 0.5 M HNO_3 concentration is sufficient to eliminate quite completely calcite as already observed with XRPD, FTIR or thermal analyses. Beyond 1 M HNO_3 concentration, the Fe content decreases strongly providing evidence that acid treatment permits the purification of raw diatomite. Aphiruk [24] has reported

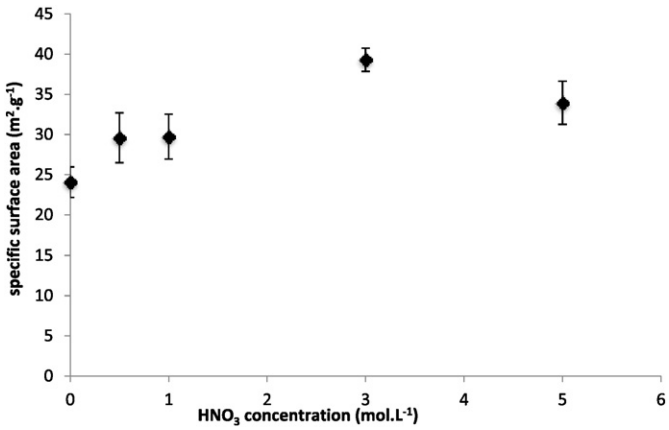

Fig. 6. Variation of specific surface area for diatomite samples treated with different nitric acid concentrations.

Table 2
Specific surface areas (a_{BET}), BET constants (C_{BET}) and density (ρ) measurements of nitric acid treated diatomite.

Samples	a_{BET}($m^2 \cdot g^{-1}$)	C_{BET}	ρ ($g \cdot cm^{-3}$)
D	24.06 ± 1.91	294.6 ± 1.0	2.2443 ± 0.0004
D-0.5 M	30.59 ± 3.64	350.4 ± 13.3	2.1876 ± 0.0001
D-1 M	29.73 ± 2.80	159.2 ± 34.0	2.187 ± 0.004
D-3 M	39.30 ± 1.45	160.4 ± 29.0	2.188 ± 0.007
D-5 M	33.94 ± 2.68	133.8 ± 22.7	2.200 ± 0.001

similar results on a Lampang (Thailand) diatomite treated with a hot 6 M H_2SO_4 solution during 24 h.

In summary, the different analyses confirm that a high-grade silica material, more than 97 wt% SiO_2 can be obtained, the carbonate impurities are quite completely eliminated with only 0.5 M HNO_3 solution at leaching time of 2 h and the Fe composition is also affected by the acid treatment which disappears progressively from 0.5 to 5 M HNO_3. Another important result is the structure of the diatomite is preserved until 5 M.

The elimination of carbonates will probably modify the density and the surface in particular the specific surface area and the porosity studied in the next paragraph.

4.1.3. BET surface area and density

As shown in Fig. 5, all the samples, the raw diatomite and the treated ones present the same nitrogen adsorption–desorption isotherm, namely a Type II isotherm, with a type H3 hysteresis loop based on the recommendation of the International Union of Pure and Applied Chemistry (IUPAC). Indeed, a small hysteresis loop can be seen in all samples but unlike Type IV isotherms, there is no plateau at high relative partial pressures p/p_0. Type II isotherms are obtained with non-porous or macroporous adsorbents, this last case concerning the diatomite. As to the small hysteresis loop, it can be explained by a change of the path followed by the desorption curve, once the condensation has occurred, due to non-rigid pores [25]. So the BJH analysis was not suitable to determine a pore size distribution or pores volumes. Tsai [26] observed the same behavior on a diatomaceous earth by using an alkaline activation.

However, comparing the influence of the acid treatment, it can be noticed that with the increase of the acid concentration until 3 M, the adsorption–desorption isotherms are shifted towards higher nitrogen adsorbed volume for each partial pressure. This phenomenon can be correlated to the increase of the specific surface area with increasing acid concentration. Fig. 6 displays the variation of the specific surface area with the increase of acid concentration. In Table 2, the specific surface areas, the BET constants and the true density according to acid concentration are reported. It appears that a_{BET} increases from 24 $m^2 \cdot g^{-1}$ for the raw diatomite to 39 $m^2 \cdot g^{-1}$ after a 3 M HNO_3 treatment. More exactly, a first increase of the specific surface area from 24 to 30 $m^2 \cdot g^{-1}$ is observed upon a treatment with low acid concentrations (0.5 or 1 M) and a second one until 39 $m^2 \cdot g^{-1}$ with a higher acid concentration (3 M). With a 5 M HNO_3, a_{BET} decreases a little bit to 34 $m^2 \cdot g^{-1}$. The first increase could be attributed to the creation of new surfaces or pores due to removal of carbonate species, emphasized by all the techniques examined previously. The decrease of the true density ρ from 2.24 to 2.20 $g \cdot cm^{-3}$ from 0.5 M concentration (Table 2) supports this explanation with the hypothesis that the carbonates have a true density higher than silica.

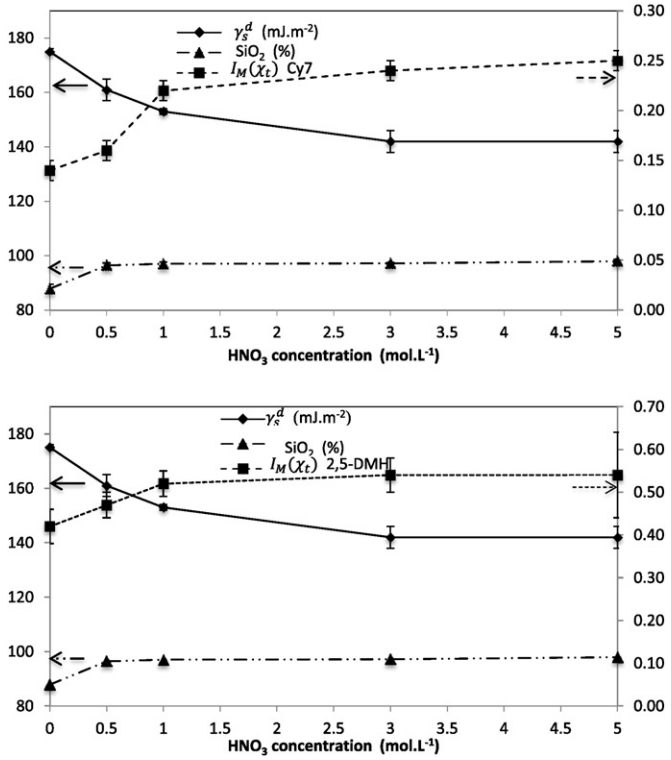

Fig. 7. Variations of the dispersive component of the surface energy γ_s^d, the nanomorphological index $I_M(\chi_t)$ for cycloheptane (cy7) and 2,5-dimethylhexane (DMH), and the silica percentage of diatomite samples versus nitric acid concentrations.

With all the carbonates being eliminated from 0.5 M, the second increase of a_{BET} noted for 1 M HNO_3 could be explained by another phenomenon, in particular the disappearance of the Fe element. Indeed, the ratio Fe/Si decreases gradually with the increase of the acid concentration (Table 1). At 5 M concentration, the specific surface area decreases probably due to a porosity covered by retained salt residues. This trend was previously observed by Tsai [26]. Boudriche [27] also noticed a decrease of the specific surface area between 3 M and 5 M on an attapulgite modified by hydrochloric acid etching.

The BET constant is also affected by the acid treatment, the disappearance of carbonates at 0.5 M concentration could explain the increase of the C_{BET}, the new surfaces revealed by the removal of carbonates having more affinity with nitrogen. In a second time the disappearance of Fe could be responsible for the decrease of the C_{BET}.

To better understand the properties of diatomite, it is important to have detailed information of the reactive sites. The surface properties of the raw and acid treated diatomite samples were examined by implementation of the IGC. This technique may be performed at infinite dilution (IGC-ID) and also at finite concentration (IGC-FC) conditions.

Table 3
Variations of the γ_s^d, $I_M(\chi_t)$ and I_{sp} values determined by IGC-ID at 100 °C, on the diatomite samples before and after treatments at different nitric acid concentrations.

	γ_s^d; ($mJ \cdot m^{-2}$)	$I_M(\chi_t)$				I_{sp} ($kJ \cdot mole^{-1}$)	
	C5, C6, C7	2,3,4-TMP	2,5-DMH	Cy7 ± 0.01	Cy8 ± 0.01	CH_2Cl_2	$CHCl_3$
D	175 ± 1	0.41 ± 0.03	0.42 ± 0.01	0.14	0.10	14.45 ± 1.66	12.30 ± 0.56
D-0.5 N	161 ± 4	0.45 ± 0.02	0.47 ± 0.03	0.16	0.12	15.47 ± 0.19	13.23 ± 0.18
D-1 N	153 ± 1	0.55 ± 0.02	0.52 ± 0.04	0.22	0.17	14.70 ± 0.27	12.46 ± 0.13
D-3 N	142 ± 4	0.56 ± 0.03	0.54 ± 0.02	0.24	0.20	14.34 ± 0.16	12.41 ± 0.29
D-5 N	142 ± 4	0.52 ± 0.06	0.54 ± 0.03	0.25	0.19	15.12 ± 0.09	12.79 ± 0.12

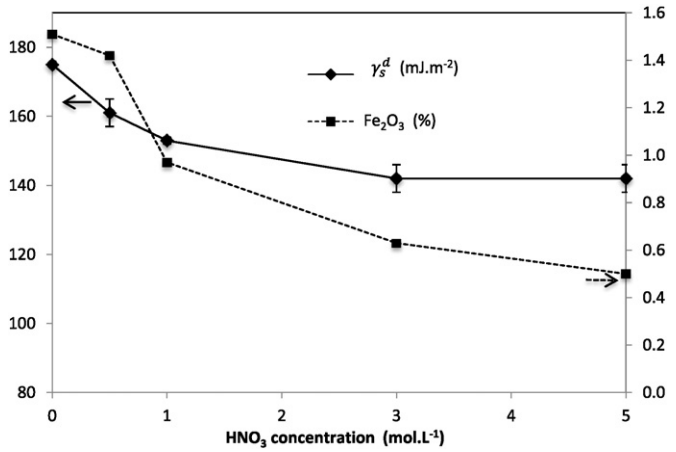

Fig. 8. Variations of the dispersive component of the surface energy, and the Fe_2O_3 percentage of diatomite samples versus nitric acid concentrations.

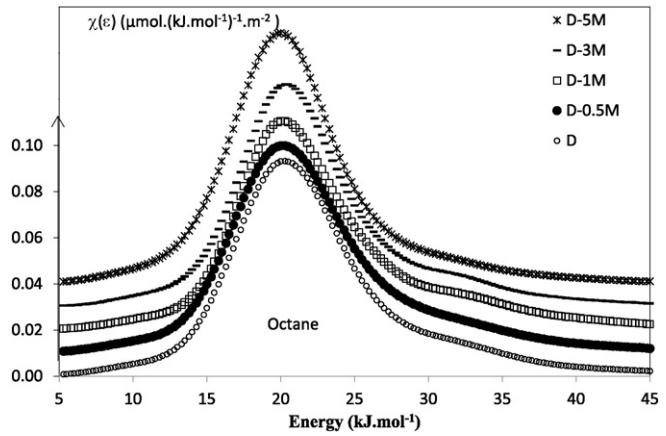

Fig. 9. Adsorption energy distribution functions of n-Octane on initial and treated diatomite samples, measured at 343 K.

4.2. Surface property characterization by IGC

4.2.1. Characterization of samples by IGC-ID

The values of different parameters measured by IGC-ID on initial and treated diatomite samples were compared (Table 3).

The value of γ_s^d decreases from 175 mJ·m^{-2} before treatment to a stable value of 142 mJ·m^{-2} after 3 M or 5 M acid treatments. At infinite dilution, the retention time is described as follow:

$$t_r = \Sigma n_i \tau_i = \Sigma n_i \tau_0 e^{E_i/RT_c} \quad (5)$$

Where n_i is the number of sites i, τ_i the residence time on the sites i, E_i the interaction energy between the probe and the sites i and τ_0 a constant.

So for a heterogeneous surface, the retention time and therefore are more influenced by higher energy sites. The decrease of γ_s^d observed with acid treatment results of the disappearance of some high energy sites.

The adsorption behaviors of branched and cyclic alkane probes were also examined by injection of 2,5-dimethylhexane (2,5-DMH), 2,3,4-triméthylpentane (2,3,4-TMP), cycloheptane (Cy7) and cyclooctane (Cy8). It could be noticed that the $I_M(\chi_t)$ increases with the increase of the acid concentration indicating the disappearance of surface roughness.

As it was already observed in previous studies [11,27], variations of γ_s^d, $I_M(\chi_t)$, and SiO_2 percentage are correlated. On the raw diatomite, the high γ_s^d value and the low $I_M(\chi_t)$ one, the former indicating the presence of high energy sites and the latter a rough surface, are both characteristic of the crystalline and morphological structure of the raw material. Under the acid treatment, the decrease of the γ_s^d and the increase of the $I_M(\chi_t)$ could result from the eliminations, not only of carbonates, but also of Fe_2O_3 as indicated by Hamdi [11] and as shown by the elementary analysis. Indeed, until 0.5 M, the values of γ_s^d and $I_M(\chi_t)$ decrease or increase respectively according to the decrease of SiO_2 percentage (Fig. 7). Above 0.5 M, this trend was roughly the same in spite of the stabilization of SiO_2 percentage, but according to the decrease of the Fe_2O_3 content (Fig. 8).

By injecting acidic probes, such as chloroform and dichloromethane, the basic character of the diatomite was assessed through the corresponding specific interaction parameters. No significant change in these parameters is observed as HNO_3 concentration increases (Table 3). Several basic probes, such as 1,4-dioxane, tetrahydrofuran and acetonitrile were injected, but due to their strong interactions with the acidic hydroxyl groups on the diatomite surface, they could not be eluted through the chromatographic column even at 473 K oven temperature, which testified the strong acidic character of the diatomite surface.

In summary, the results obtained by IGC-ID analyses demonstrate that the surface properties are influenced by the acid treatment. The highest variations are obtained with the dispersive component of the surface energy and with the nanomorphological index and both values are obtained with apolar probes that is to say alkanes. The variation of the specific component obtained with polar probe is lower.

The IGC-ID parameters are clearly related to the adsorption sites having the highest energy of interaction [19]. The IGC-FC analysis was then used to provide information on the whole surface.

4.2.2. Characterization of samples by IGC-FC

4.2.2.1. Study of the isotherm desorption. The raw and acid treated diatomite samples were submitted to IGC-FC using an apolar probe, octane, which is mainly sensitive to surface morphology, and two polar probes, isopropanol and 1,4-dioxane, more sensitive to the surface functionality, especially the presence of silanol groups. The specific surface areas, the corresponding BET constants and irreversibility indexes determined with these three probes are collected in Table 4. The irreversibility index I_{irr} provides an estimate of the proportion of high energy sites depending on the nature of the probe.

Table 4
Comparison of specific surface areas (a_{BET}), BET constant (C_{BET}) and irreversibility indexes ($Iirr$) of diatomite treated at different nitric acid concentrations, which are obtained by nitrogen adsorption and IGC-FC.

	C8 (70 °C)			IP (50 °C)			DX (60 °C)		
	a_{C8} (m^2·g^{-1})	C_{BET}	I_{irr} (%)	a_{IP} (m^2·g^{-1})	C_{BET}	I_{irr} (%)	a_{DX} (m^2·g^{-1})	C_{BET}	I_{irr} (%)
D	26.3 ± 0.3	8	1.5 ± 0.1	28.0 ± 1.0	13.2	19.9 ± 2.3	26.8 ± 0.7	10	7.1 ± 0.1
D-0.5 M	30.9 ± 0.1	8	1.9 ± 0.2	34.5 ± 0.3	13.4	19.8 ± 1.5	32.7 ± 0.1	11	7.2 ± 0.1
D 1 M	34.8 ± 0.1	9	0.9 ± 0.1	34.7 ± 0.5	12.7	21.6 ± 1.3	38.0 ± 0.1	10	9.7 ± 0.1
D-3 M	45.3 ± 0.1	8	1.0 ± 0.1	49.9 ± 0.5	12.9	21.0 ± 1.1	44.7 ± 1.0	10	9.7 ± 1.0
D-5 M	45.8 ± 0.1	7	0.7 ± 0.1	36.1 ± 0.6	11.9	22.9 ± 1.2	43.0 ± 0.3	9	11.5 ± 0.9

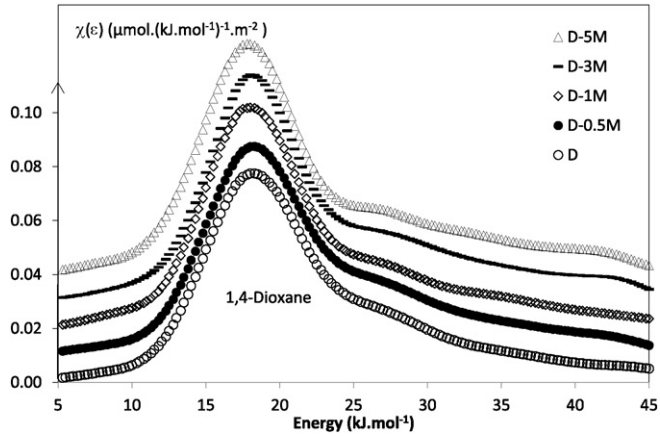

Fig. 10. Adsorption energy distribution functions of 1,4-dioxane on initial and treated diatomite samples, measured at 333 K.

The specific surface areas measured by IGC-FC are slighly higher than those obtained by nitrogen. Balard [20] noticed the same behavior on milled graphites and attributed it to the occupied area by organic probes. Indeed, the surrounding seems to influence the conformation of the probe adsorbed on the solid surface. So the real cross sectional area of the probe in its adsorbed state is not exactly the theoretical one, leading to the overestimation of the specific surface area.

When comparing the influence of the acid concentration, the specific surface areas increase until the 3 M whatever the probe is. The same variation was already observed after an acid treatment on an attapulgite clay [27]. As previously said with N_2 adsorption, it is explained by the removal of carbonates and metallic oxides like Fe_2O_3 inducing appearance of new surfaces. Beyond the 3 M concentration, the variation of specific surface area value depends on the nature of the probe. It decreases for isopropanol and 1,4-dioxane as for nitrogen probably due to the surface coverage by retained salt residues.

The BET constants obtained with organic probes are not so much sensitive to the acid treatment compared to nitrogen and are much weaker. This behavior can be attributed to the analysis that temperature is higher with organic probes (323–343 K) than with nitrogen (77 K), the interactions between a probe and the solid surface being favored at lower temperatures.

But it could be noticed that BET constants are sensitive to the polarity of the probe, the BET constants are higher with isopropanol or 1,4-dioxane than with octane, emphasizing a better affinity of polar probes towards the surface than the apolar one. This result can be explained by the structure of the diatomite composed of polar silanol groups. With organic probes, the irreversibility index I_{irr} shows the same trends than with BET constants, the highest ones are obtained with isopropanol (nearby 20%). Isopropanol interacts more strongly with both silanol and siloxane groups on the diatomite or silica surface formed at high acid concentrations. The I_{irr} obtained with 1,4-dioxane is lower than with isopropanol. Indeed, 1,4-dioxane, a basic probe, exhibits affinity only with acid groups like silanols, as previously observed by Kellou [28] on dimethyl silylated silicas. Comparing the influence of the acid concentration on the I_{irr} obtained with 1,4-dioxane and isopropanol, the variations are similar to those observed by Boudriche [27] on the Algerian attapulgite. They increase with the increase of acid concentration emphasizing that acid treatment purifies the surface and reveals silanol groups.

The modifications of the surface heterogeneity according to the increase of the acid concentration will be also assessed through the distribution functions of the adsorption energies (DFAE) of the organic probes.

4.2.2.2. Variation of the surface energetic heterogeneity. The surface heterogeneity of the samples was evaluated by determining the distribution functions of adsorption energies (DFAE) of the three organic probes, octane, isopropanol and 1,4-dioxane. The DFAE were computed according to the method of Rudzinski and Jagiello [22], by applying the technique of multiple derivations developed by Balard [18,19]. On all figures presented, the DFAE obtained with the different acid concentrations (Figs. 9–11) were moved on the ordinate ax for a better readability.

The DFAE of n-octane obtained on samples treated with the different HNO_3 concentrations are compared in Fig. 9. This probe leads to a DF quite monomodal with a peak centered on 20 kJ/mol and almost superposable for all the studied samples. This apolar probe, only sensitive to the morphology changes on the surface, testifies that no important morphology modification takes place after acid treatment. In other words, the surface modifications revealed at very low surface coverage by IGC-ID are not observed when the monolayer is reached (IGC-FC).

The DFAE of the 1,4-dioxane are slightly different than those obtained with octane. Indeed, they are quite monomodal with a maximum of

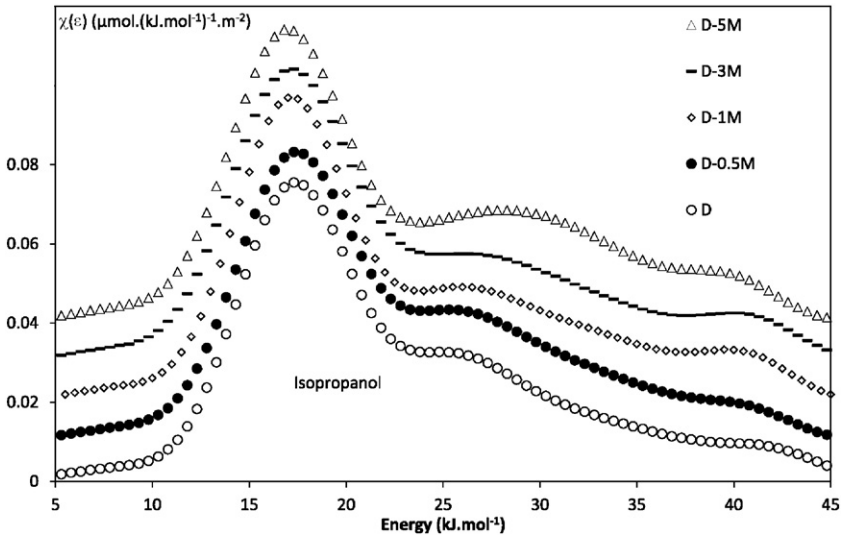

Fig. 11. Adsorption energy distribution functions of isopropanol on initial and treated diatomite samples, measured at 323 K.

Table 5
Heterogeneity index (*Ihete*) values, measured by IGC-FC for n-octane, isopropanol and 1,4-dioxane probes, on raw and treated diatomite.

	I_{hete} (%)		
	C8	IP	DX
D	28.2 ± 0.1	47.7 ± 0.1	36.8 ± 1.3
D-0.5 M	25.8 ± 1.0	46.3 ± 0.1	37.4 ± 1.2
D-1 M	28.0 ± 0.6	46.6 ± 0.6	37.7 ± 2.7
D-3 M	26.4 ± 2.0	45.4 ± 0.6	35.1 ± 1.5
D-5 M	17.6 ± 4.4	43.3 ± 2.2	32.7 ± 2.0

the main peak located at 18–19 kJ/mol and an important tail extending towards the high energies up to 45 kJ/mol (Fig. 10). The 1,4-dioxane, a basic probe, is sensitive to the functionality of the surface and can establish strong specific interactions with acidic sites like silanols. The different kinds of silanol groups (single or germinal, H-bonded or isolated ones) can lead to the observed asymmetrical peak. Considering the acidic treatment, this one doesn't affect the shape of the distribution functions, that is to say the presence of the acidic groups, testifying the stability of the silanol groups towards the acidic treatment in the point of view of the 1,4-dioxane.

By its ability to exchange interactions through hydrogen bounding, the isopropanol is also sensitive to the surface functionality. Fig. 11 displays the FDAE determined on diatomite using isopropanol according to the acidic treatment. All heterogeneity curves show a first peak with a maximum located at 18–19 kJ/mol followed by a second one at high energies between 25 and 30 kJ/mol. This last one is more pronounced with the D-5 M treated sample. This FDAE clearly bimodal and very similar to those exhibited by pyrogenic silicas, reflects the transformation of the diatomite towards a silica structure as showed by XRF. According to Balard [29,30], pyrogenic silicas exhibit two types of energy sites on the surface leading to two peaks: a peak at lower energy bound corresponds to non-specific interactions between siloxane bridges and the isopropanol probe whereas the peak at high energy corresponds to strong interactions through hydrogen bond between alcohol function of isopropanol and silanol groups on the solid. This attribution was supported by variations of the DF determined for two pyrogenic silicas submitted to a silylation [29].

The asymmetry of the FDAE can describe the surface heterogeneity by means of an index of heterogeneity (I_{hete}). The values were determined for n-octane, isopropanol and 1,4-dioxane probes (Table 5). The indexes of heterogeneity of isopropanol and 1,4-dioxane are much greater than those of n-octane, because polar probes interact more strongly with the surface functional groups through hydrogen bounds.

The indexes decrease a little bit with HNO_3 concentration indicating again a purification and a change towards a more chemically homogeneous surface.

5. Conclusion

The objective of this study of a diatomite upon an acid treatment was to correlate its structural and chemical properties determined by different techniques (SEM, XRD, XRF, FTIR, ATG, nitrogen adsorption) with surface properties investigated by IGC.

Decarbonation upon the acid treatment led to an increase of the specific surface area, an important property for the use of diatomite as catalyst support with a respect of the morphology and the crystal structure of the diatomite.

The IGC-ID showed that the variations of the dispersive surface component and of the nanomorphological index were correlated with the change from diatomite to quite pure silica.

By IGC-FC, the distribution function obtained with n-octane, a probe sensitive to the surface morphology, remained unchanged with acid treatment indicating the stability of the morphology. On the contrary, the distribution function obtained with isopropanol, a probe sensitive to chemical functionality, confirmed the modification of the diatomite towards a silica structure, exhibiting two types of energy sites: the first type is those sites at lower energy corresponding to siloxane bridges and the second type is those at higher energy compared to the silanol groups of great interest for adsorption of organic pollutants.

Thus, IGC has enabled us to gather information about the surface properties of diatomite cleaned with nitric acid. Among these is its interactive potential with organic probes, which is interesting in order to use diatomite as a catalyst support for the removal of organic pollutants by photodegradation.

References

[1] E. Erden, G. Çölgeçem, R. Donat, The removal of textile dyes by diatomite earth, J. Colloid Interface Sci. 282 (2005) 314–319.
[2] M.A.M. Khraisheh, M.A. Al-Ghouti, S.J. Allen, M.N. Ahmad, Effect of OH and silanol groups in the removal of dyes from aqueous solution using diatomite, Water Res. 39 (2005) 922–932.
[3] R. Goren, T. Baykara, M. Marsoglu, Effects of purification and heat treatment on pore structure and composition of diatomite, Br. Ceram. Trans. 101 (2002) 177–180.
[4] X. Wang, S. Gao, L. Yu, C. Miao, Synthesis of porphyrin nanometer material by a new method, Chem. J. Chin. Univ. 19 (1998) 854–857 (in Chinese).
[5] Y. Su, Y. Yu, P. Yang, X. Wang, X. Zhu, Photocatalytic degradation of antraquinone dye wastewater with nano-TiO_2/diatomite, China Environ. Sci. 29 (2009) 1171–1176.
[6] C.N. Satterfield, Heterogeneous catalysis in practice, McGraw-Hill, 1980 221 (Chap. 4).
[7] P. Yuan, D.Q. Wu, H.P. He, Z.Y. Lin, The hydroxyl species and acid sites on diatomite surface: a combined IR and Raman study, Appl. Surf. Sci. 227 (2004) 30–39.
[8] D.L. Trimm, A. Stanislans, The control of pore size in alumina catalyst supports: A review, Appl. Catal. 21 (1986) 215–238.
[9] D.L. Trimm, Design of Industrial Catalysts, Chemical Engineering Monographs 11, Elsevier, Amsterdam, 1980 91.
[10] L. Boudriche, B. Hamdi, Z. Kessaissia, R. Calvet, A. Chamayou, J.A. Dodds, H. Balard, An assessment of the surface properties of milled attapulgite using inverse gas chromatography, Clay Clay Miner. 58 (2010) 143–153.
[11] B. Hamdi, Z. Kessaissia, J.B. Donnet, T.K. Wang, IGC characterization of surface energy and morphology of two natural fillers: kieselguhr and bentonite, Ann. Chim. Sci. Mater. 25 (2000) 481–494.
[12] X. Huang, B. Li, B. Shi, L. Li, Investigation on interfacial interaction of flame retarded and glass fiber reinforced PA66 composites by IGC/DSC/SEM, Polymer 49 (2008) 1049–1055.
[13] M.G. Cares-Pacheco, R. Calvet, G. Vaca-Medina, A. Rouilly, F. Espitalier, Inverse gas chromatography a tool to follow physicochemical modifications of pharmaceutical solids: crystal habit and particles size surface effects, Int. J. Pharm. 494 (2015) 113–126.
[14] L. Boudriche, A. Chamayou, R. Calvet, B. Hamdi, H. Balard, Influence of different dry milling processes on the properties of an attapulgite clay, contribution of inverse gas chromatography, Powder Technol. 254 (2014) 352–363.
[15] J.R. Conder, C.L. Young, Physicochemical measurements by gas chromatography, Wiley Interscience, New York, 1979 385–390.
[16] H. Balard, Estimation of the surface energetic heterogeneity of a solid by inverse gas chromatography, Langmuir 13 (1997) 1260–1269.
[17] G.M. Dorris, D.G. Gray, Adsorption spreading pressure and London force interactions of hydrocarbons on cellulose and wood fiber surfaces, J. Colloid Interface Sci. 71 (1979) 93–104.
[18] E. Brendlé, E. Papirer, A new topological index for molecular probes used in inverse gas chromatography for the surface nanorugosity evaluation. 1. Method of evaluation, J. Colloid Interface Sci. 194 (1997) 207–216.
[19] H. Balard, E. Brendlé, E. Papirer, Determination of the acid–base properties of solid surfaces using inverse gas chromatography: advantages and limitations, in: K. Mittal (Ed.), Acid–Base Interactions, Relevance to Adhesion Science and Technology VSP, Utrecht, the Netherlands 2000, pp. 299–316.
[20] H. Balard, D. Maafa, A. Santini, J.B. Donnet, Study by inverse gas chromatography of the surface properties of milled graphites, J. Chromatogr. A 1198-1199 (2008) 173–180.
[21] W. Rudzinski, D.H. Everett, Adsorption of Gases on Heterogeneous Surfaces, Academic Press, London, 1992.
[22] W. Rudzinski, J. Jagiello, Y. Grillet, Physical adsorption of gases on heterogeneous solid surface: evaluation of the adsorption energy distribution from adsorption isotherms and heats of adsorption, J. Colloid Interface Sci. 87 (1982) 478–491.
[23] P. Falaras, I. Kovanis, F. Lezou, G. Seiragakis, Cottonseed oil bleaching by acid-activated montmorillonite, Clay Miner. 34 (1999) 221–232.
[24] A. Chaiserna, K. Rangsriwatananon, Effects of thermal and acid treatments on some physico-chemical properties of lampang diatomite, J. Sci. Technol. 11 (2004) 289–299.
[25] F. Rouquerol, J. Rouquerol, K. Sing, Adsorption by Powders and Porous Solids, second ed. Academic Press, London, 1999.

[26] W.-T. Tsai, K.-J. Hsien, C.-W. Lai, Chemical Activation of Spent Diatomaceous Earth by Alkaline Etching in the Preparation of Mesoporous Adsorbents, Ind. Eng. Chem. Res. 43 (2004) 7513–7520.
[27] L. Boudriche, R. Calvet, B. Hamdi, H. Balard, Effect of acid treatment on surface properties evolution of attapulgite clay: An application of Inverse Gas chromatography, Colloids Surf. A Physicochem. Eng. Asp. 392 (2011) 45–54.
[28] H. Kellou, B. Hamdi, E. Brendlé, T. Gottschalk-Gaudig, H. Barthel, H. Ridaoui, H. Balard, J.B. Donnet, Surface properties of dimethyl silylated silicas, assessed using IGC at finite concentration, Colloids Surf. A Physicochem. Eng. Asp. 327 (2008) 90–94.
[29] J.B. Donnet, Y.J. Li, T.K. Wang, H. Balard, G.T. Burns, Surface energy of silica Xerogels and Fumed silica by Inverse Gas chromatography and Inverse liquid chromatography, Rubber Chem. Technol. 75 (2002) 811–824.
[30] H. Balard, E. Papirer, A. Khalfi, H. Barthel, in: J. Weis, N. Auner, J. Weis (Eds.), Organosilicon IV: from Molecules to Materials, Wiley, Weinheim 2000, pp. 773–792.